RADIO SCIENCE, VOL. 38, NO. 4, 8078, doi:10.1029/2002RS002729, 2003

Retrieval of sea surface wind vectors from simulated satellite microwave polarimetric measurements

Quanhua Liu[1]
Cooperative Institute of Research in the Atmosphere, Colorado State University, Boulder, Colorado, USA

Fuzhong Weng
NOAA/NESDIS Office of Research and Applications, Camp Springs, Maryland, USA

Received 30 May 2002; revised 30 August 2002; accepted 17 September 2002; published 31 July 2003.

[1] An algorithm is developed to retrieve sea surface wind vectors from satellite microwave polarimetry. The radiative transfer model produces simulated measurements under global atmospheric and surface conditions. The simulations for wind speeds less than 5 m s^{-1} are not utilized in the retrievals because of the unreliable performance of the current surface emissivity model. In the algorithm, the upwelling and downwelling radiative components are treated as one variable since the two components are highly correlated. As a result, under rain-free conditions, the full polarimtric measurements obtained at a single frequency can form a closure of a set of radiative transfer equations so that both surface and atmospheric column parameters can be simultaneously derived. The first guess to the solutions is normally required because the retrieval is nonlinear. In doing so, the third and fourth Stokes components and their ratio are utilized to estimate the wind direction. It is found that this ratio alone can determine the wind direction with an accuracy of 30 degrees. Without the sensor noises being added to the simulations, the algorithm can produce the wind direction with an RMS error of 6.5 degrees and the wind speed with an error of 0.3 m s^{-1}, respectively. If the realistic random noises are taken into account with 0.1 K for vertical and horizontal polarizations and 0.15 K for the third and fourth Stokes components, the errors increase to about 10 degrees and 0.6 m s^{-1} for the wind direction and speed, respectively. This wind speed error is much smaller than that from the statistical algorithms (1.4 m s^{-1}) applied for the same data set. Thus the physical retrieval significantly improves the uses of the microwave polarimetric data for remote sensing of ocean wind. *INDEX TERMS:* 3360 Meteorology and Atmospheric Dynamics: Remote sensing; 3367 Meteorology and Atmospheric Dynamics: Theoretical modeling; *KEYWORDS:* polarimetric signature, surface wind, retrieval

Citation: Liu, Q., and F. Weng, Retrieval of sea surface wind vectors from simulated satellite microwave polarimetric measurements, *Radio Sci.*, *38*(4), 8078, doi:10.1029/2002RS002729, 2003.

1. Introduction

[2] Accurate information on the sea surface state such as wind vector is of great importance for modeling the air-sea interaction in weather and climate models. Therefore many remote sensing algorithms have been developed to retrieve the surface wind speed. With the Special Sensor/Microwave Imager (SSM/I) and collocated buoy data, *Goodberlet et al.* [1990] derived a simple regression algorithm using all seven SSM/I channels. *Wentz* [1992] also developed an algorithm to derive the wind direction with the weather model wind vectors as a first guess. Recently, *Yueh et al.* [1999], *Yueh and Wilson* [1999], and *Meissner and Wentz* [2002] also analyzed and confirmed the correlation between the microwave polarimetric signatures and the surface wind direction.

[3] The future passive microwave sensors such as the U.S. Navy WindSAT/Coriolis and U.S. National Polar-

[1]Now at NOAA/NESDIS, Camp Springs, Maryland, USA.

0048-6604/03/2002RS002729

Orbiting Environmental Satellite System (NPOESS) Conical Microwave Imager Sounder (CMIS) are all developed with the polarimetric sensors for global remote sensing of surface wind vectors. The retrieval of the surface wind speed can be improved beyond the SSM/I performance by deriving the speed and direction simultaneously. In doing so, a physical algorithm often derives the state of the atmospheric parameters through iterations until the simulated radiances by the forward radiative transfer model converge to the measurements within a predefined error margin [*Schmetz and Turpeinen*, 1988; *Kummerow et al.*, 1989; *Weng and Grody*, 2000]. Since the retrieval of the sea surface wind direction is a nonlinear problem and the variation of the polarimetric signatures due to the wind direction is less than a few degrees in kelvins, the radiative transfer model must be developed very accurately. As an example, a fast and accurate polarimetric surface emissivity model is yet to be developed and to be utilized in the retrieval [*Yueh*, 1997; *Gasiewski and Kunkee*, 1994], while a number of accurate polarimetric atmospheric radiative transfer model have been developed and validated [*Weng*, 1992; *Haferman et al.*, 1993; *Liu et al.*, 1996].

[4] This study proposed a parameterized forward model and its tangent linear model that can be directly used in the ocean wind vector retrieval. The algorithm is tested with simulated measurements. In section 2, the physical base of the algorithm is described. A sensitivity of Stokes components to wind speed and direction is studied in section 3. The algorithm performance and discussion are given in sections 4 and 5, respectively.

2. Retrieval Algorithm

[5] The philosophy of the physical retrieval algorithm is to derive a surface/atmospheric state whose corresponding simulated brightness temperatures are in agreement with the measured brightness temperatures. Since satellite measurements are subject to noise and there is a slight inconsistency between simulations and measurements, an agreement can only be achieved within a certain threshold. *Piepmeier and Gasiewski* [2001] have studied the retrieval of the wind vector from the multifrequencies and multiple looking angles' measurements. They retrieved wind speed and direction separately. The algorithm developed in this study derived the wind speed and direction simultaneously. A Stokes vector at a single frequency and at a single looking azimuthal angle is used to calculate the wind vector. The first guess of wind direction is obtained from the ratio of the third to fourth Stokes components. The algorithm is tested against the simulated polarimetric measurements for a global ocean/atmosphere data set.

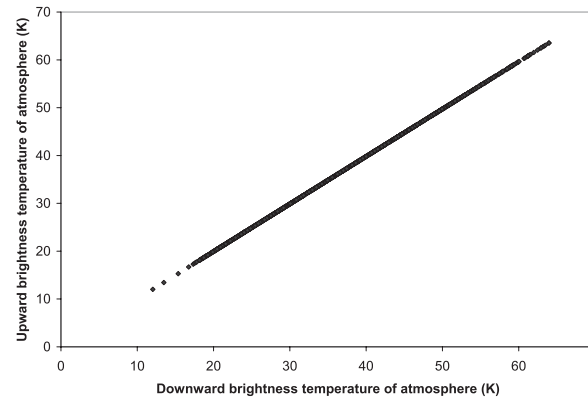

Figure 1. Upward atmospheric radiation versus downward atmospheric radiation. The viewing zenith angle is 53°.

[6] For an atmosphere in the absence of scattering and having an emission azimuthally independent, the radiative transfer equation can be expressed as

$$T_v = \varepsilon_v \tau T_s + T_u + \tau(1-\varepsilon_v)T_d \quad (1)$$

$$T_h = \varepsilon_h \tau T_s + T_u + \tau(1-\varepsilon_h)T_d \quad (2)$$

$$U = \varepsilon_3 \tau T_s \quad (3)$$

$$V = \varepsilon_4 \tau T_s, \quad (4)$$

where T_S is the sea surface temperature, τ is the atmospheric transmittance, T_u and T_d are the upward and downward atmospheric radiation, respectively, and ε_v, ε_h, ε_3, ε_4 are the sea surface emissivity for the vertically polarized, horizontally polarized, and the third and the fourth Stokes components respectively. The first, second, and third terms on the right-hand sides of equations (1) and (2) are the contributions from the surface emission, upward atmospheric radiation, and from surface reflected downward atmospheric radiation, respectively. The third and fourth Stokes components from the atmosphere vanish due to the zero or small single scattering albedo at low frequency and the azimuthal symmetry. Therefore the third and fourth Stokes components are only contributed by the surface, and they are attenuated by the atmosphere.

[7] In equations (1)–(4), T_s, τ, T_u, T_d, wind speed s, and wind direction ϕ are six unknown parameters. Sea surface temperature can be obtained from the operational sea surface temperature product [*Reynolds and Roberts*, 1987]. Therefore sea surface temperature is treated as a

known variable. The upward and downward atmospheric radiations are almost identical (see Figure 1) with 0.99 of the correlation coefficient and 0.2 K of maximum difference, and they are denoted by T_a hereinafter. The high correlation is due to the fact that the most water vapor locates near the surface, which reduces the difference between the sea surface temperature and the effective atmospheric temperature. In addition, atmospheric radiation is not sensitive to the vertical distribution of the atmospheric temperature because the absorption coefficient decreases slightly with the temperature. Thus the six unknown parameters are reduced to four unknown parameters, which lead to a closure in the physical inversion.

[8] The physical inversion method has been successfully applied for the retrieval of the vertical profiles of the atmospheric temperature and moisture [*Chedin et al.*, 1985; *Smith et al.*, 1992]. *Kummerow et al.* [1989] developed a physical inversion method for the retrieval of rain rate from the microwave measurement. A physical inversion algorithm dealing with the total precipitable water, cloud liquid water, and sea surface wind speed has also been developed [*Liu and Simmer*, 1998]. In this paper, we extend the physical inversion algorithm to the retrieval of the sea surface wind vector. On the basis of equations (1)–(4), the inversion equations can be represented by

$$\begin{bmatrix} \Delta s \\ \Delta\phi \\ \Delta\tau \\ \Delta T_a \end{bmatrix} = (\mathbf{A}^t\mathbf{A} + \mathbf{E})^{-1}\mathbf{A}^t \begin{bmatrix} \Delta T_v \\ \Delta T_h \\ \Delta U \\ \Delta V \end{bmatrix}, \qquad (5)$$

where

$$\mathbf{A} = \begin{bmatrix} \tau(T_s - T_a)\dfrac{\partial \varepsilon_v}{\partial s} & \tau(T_s - T_a)\dfrac{\partial \varepsilon_v}{\partial \phi} & T_a(1-\varepsilon_v) + T_s\varepsilon_v & 1 + \tau(1-\varepsilon_v) \\ \tau(T_s - T_a)\dfrac{\partial \varepsilon_h}{\partial s} & \tau(T_s - T_a)\dfrac{\partial \varepsilon_h}{\partial \phi} & T_a(1-\varepsilon_h) + T_s\varepsilon_h & 1 + \tau(1-\varepsilon_h) \\ \tau T_s\dfrac{\partial \varepsilon_3}{\partial s} & \tau T_s\dfrac{\partial \varepsilon_3}{\partial \phi} & T_s\varepsilon_3 & 0 \\ \tau T_s\dfrac{\partial \varepsilon_4}{\partial s} & \tau T_s\dfrac{\partial \varepsilon_4}{\partial \phi} & T_s\varepsilon_4 & 0 \end{bmatrix}. \qquad (6)$$

The superscript t in equation (5) refers to the transpose of the matrix. Matrix **E** represents an error matrix depending on the measurement error and other errors.

[9] The inversion equation can be solved using an iterative method. For a set of measurement, the modeled Stokes vector can be obtained through equations (1)–(4) for the given atmospheric and surface parameters. Matrix **A** can be also calculated based on the given parameters. The difference between the modeled data and measurements is then used to determine the change of the atmospheric and surface parameters. The iteration goes on until it converges.

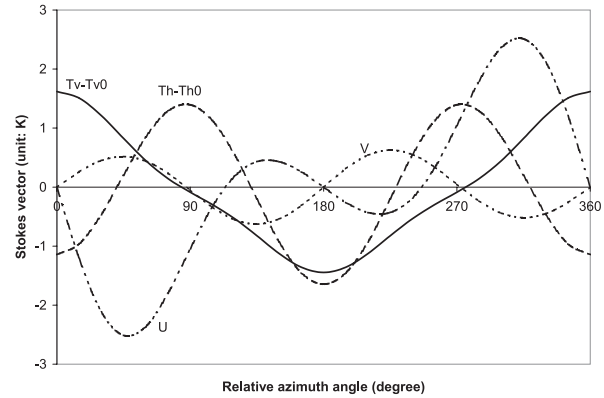

Figure 2. Variation of Stokes vector at 37 GHz with the relative azimuth angle for wind speed of 10 m s^{-1} and the sea surface temperature of 300 K. The averaged values for the horizontally and vertically polarized brightness temperatures are extracted. The dashed, solid, dash-dotted, and dotted lines denote the horizontally polarized, vertically polarized, and the third and fourth Stokes components, respectively. The viewing zenith angle is 53°.

3. Sensitivity Study

[10] The variation of Stokes vector to the wind direction is generally less than 3 K (Figure 2). The amplitudes of the variation for the vertically and horizontally polarized components are about 2 K. The amplitudes of the variation are about 3 and 0.5 K for the third and the fourth components of Stokes vector, respectively. For the retrieval of the wind direction, the algorithm deals with the small signatures. The retrieval error of the sea surface wind vector mainly relates to the measurement error of Stokes vector. The measurement error is mainly composed of the calibration error and the radiometric noise. The absolute radiometric accuracy is defined as a difference between the brightness temperature values as measured by the sensor when compared to a standard calibration target. The calibration accuracy affects directly the retrieval accuracy of the geophysical parameters, especially the systematic bias. *Hollinger et al.* [1990] studied the absolute calibration error of SSM/I by comparing the brightness temperatures from satellite measurements and from SSM/I simulator measurements.

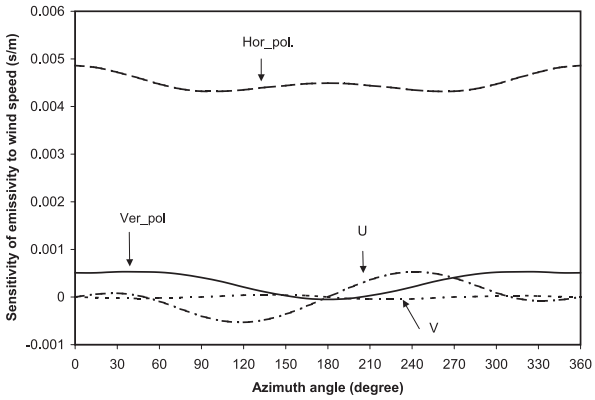

Figure 3. Derivation of emissivity to sea surface speed at 10 m s^{-1}at 37 GHz and the surface temperature of 300 K. The dashed, solid, dash-dotted, and dotted lines represent the horizontally polarized, vertically, polarized, and the third and fourth Stokes components, respectively. The viewing zenith angle is 53°.

They also compared the brightness temperatures from satellite measurements to those calculated using theoretical models. The absolute brightness temperature calibration of the SSM/I may be better than ±3 K. A great effort has been made for Special Sensor Microwave Imager Sounder (SSMIS) instrument. The absolute calibration error of SSMIS is believed to be better than ±1 K.

[11] A stable calibration is more important for retrieval algorithms. The vicarious calibration may allow for removing the biases due to the instrument degradation as it is deployed for the ground-based and airborne sensors by making simultaneous radiometric measurements over spatially and spectrally homogeneous Earth targets [*Butler and Barnes*, 1998] (see also http://eospso.gsfc.nasa.gov/calibration). The vicarious method has also been applied to SSM/I sensor for the bias correction [*Simmer*, 1994]. Thus this study did not take into account the bias because it will be removed by the vicarious calibration.

[12] The instrumental noise or radiometric noise is the standard deviation of the radiometer output referenced to the energy of the radiation incident on the antenna. It depends on the system noise temperature, receiver noise temperature, scene antenna temperature, bandwidth, radiometer integration time, and RMS radiometer gain fluctuation and drift. The instrumental noise is random and cannot be removed. The noise has the biggest impact on the convergence and accuracy of the physical retrieval. However, the sensitivity to different algorithms is different. From equations (3) and (4), the relative change of the third and the fourth components can be represented (the effect due to the error in the sea surface temperature on the emissivity is negligible) as

$$\frac{\Delta U}{U} = \frac{\Delta T_s}{T_s} + \frac{\Delta \tau}{\tau} + \frac{\Delta \varepsilon_3}{\varepsilon_3}, \tag{7}$$

$$\frac{\Delta V}{V} = \frac{\Delta T_s}{T_s} + \frac{\Delta \tau}{\tau} + \frac{\Delta \varepsilon_4}{\varepsilon_4} \tag{8}$$

The effect of the first term on the right-hand sides of equations (7) and (8) is less than 0.2% for an error of 0.5 K for the sea surface temperature. The effect of the second term is generally less than 1%, which corresponds to about 10% error of the water vapor for the transmittance at 37 GHz or 20% error of the water vapor for the transmittance at 10.7 GHz. Thus the first and the second terms are negligible. Therefore the relative changes of the third and the fourth components of Stokes vector are mainly determined by their surface emissivities, which are a function of wind vector for given frequency and surface temperature.

[13] The horizontally polarized brightness temperature is sensitive to the sea surface wind speed. The change of the wind speed of 1 m s^{-1} results in about 1 K change in the horizontally polarized brightness temperature. The sensitivity of the vertically polarized brightness temperature, the third and the fourth Stokes parameters to the wind speed is very small (Figure 3). All Stokes components are sensitive to the wind direction (Figure 4) although the third component of Stokes vector has the largest amplitude.

4. Results

[14] The results presented here are based on the simulated polarimetric data. The polarimetric two-stream radiative transfer model [*Liu and Weng*, 2002] is applied

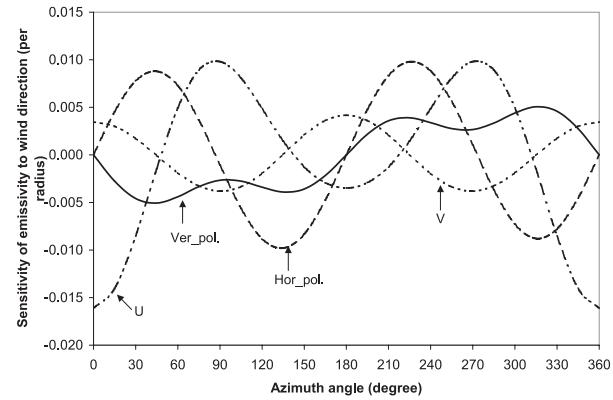

Figure 4. Same as Figure 3, but for the derivation of emissivity to sea surface wind direction.

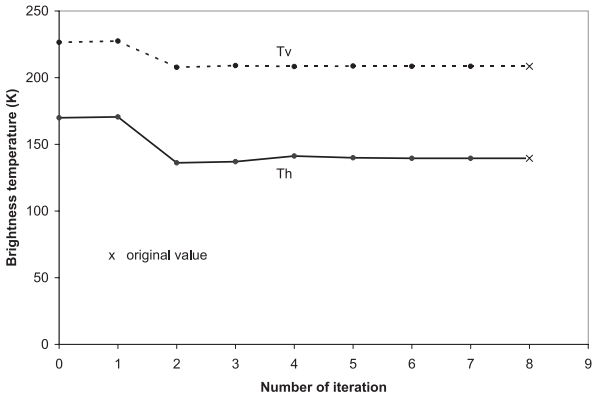

Figure 5. Convergence of the horizontally and vertically polarized brightness temperatures with the number of iteration. The crosses represent the original or true value. The viewing zenith angle is 53°.

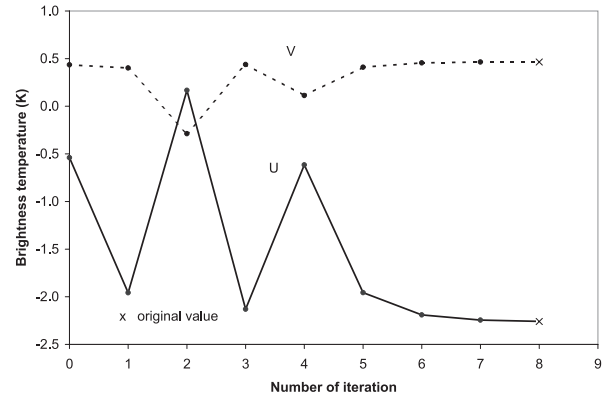

Figure 6. Same as Figure 5, but for the third and fourth Stokes components.

to simulate the polarimetric microwave data for a global data set. Polarimetric surface emissivity model [*St. Germain and Poe*, 1998], developed by U.S. Naval Research Laboratory fitting the surface measurements, is used. The emission model is an empirical model. The inputs of the model are the sea surface wind speed and direction as well as the sea surface temperature. The predicted values of the model are the surface emitted brightness temperatures in the vertical and horizontal polarization, the third and the fourth components of Stokes vector. The parameters are converted to the surface emissivities by dividing the sea surface temperature. The surface emissivities for the vertical and horizontal polarization are expanded into three harmonic cosine series. The third and the fourth components of the emissivities are expanded into three harmonic sine series. The expansion coefficients are a function of the wind speed and are calculated from measurements. The surface measurements are carried out for a viewing angle of 53 degrees and for frequencies at 6.8, 10.7, 19.35, and 37 GHz. The viewing angle and frequencies are close to those of WindSAT and CMIS. The horizontally polarized brightness temperature contains the most signatures for the sea surface wind speed (Figure 3). The vertically polarized brightness temperature can be used for determining the atmospheric effect because its variations to the wind speed and direction are much smaller than its variation to the atmospheric variation (see Figure 1). The third component of Stokes vector is sensitive to the sea surface wind direction (see Figure 4). The fourth component of Stokes vector can be used to reduce the ambiguity in determining the sea surface wind direction. The physical retrieval algorithm is first applied for noiseless data. A tropical atmospheric profile with a sea surface speed of 10 m s^{-1} at a relative direction of 45° is used in the simulation. Figures 5–7 show the convergence process of the vertically and horizontally polarized brightness temperature (Figure 5), the last two Stokes components (Figure 6), and the sea surface wind speed and direction (Figure 7). The convergence of the first two components of the Stokes vector is faster than the last two components because the relative change of the first two components is smaller. The convergence of the case is achieved after five iterations. However, the solution of the inversion problem may not be unique, especially when the radiometric noise is introduced. A good first guess may be helpful to avoid the ambiguous solutions. The regression equation developed by *Goodberlet et al.* [1990] for sea surface wind speed and the regression equation developed by *Petty* [1994] for the total precipitable water have been applied to obtain the parameters for the first guess. The RMS error of the regression methods for the simulated data

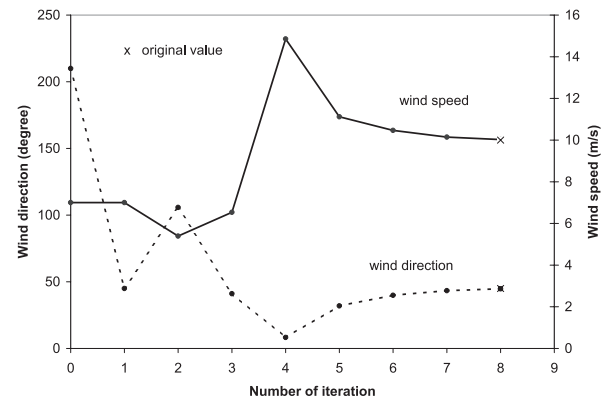

Figure 7. Convergence of the sea surface wind speed and direction with the number of iteration. The crosses represent the original or true value. The viewing zenith angle is 53°.

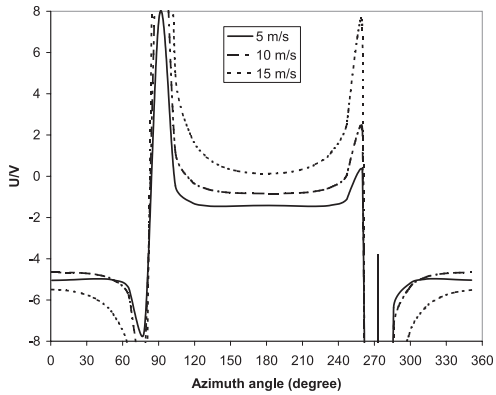

Figure 8. Criterion for the region of the azimuth angle. The solid, dash-dotted, and dotted lines are for wind speed of 5, 10, and 15 m s^{-1}, respectively. The viewing zenith angle is 53°.

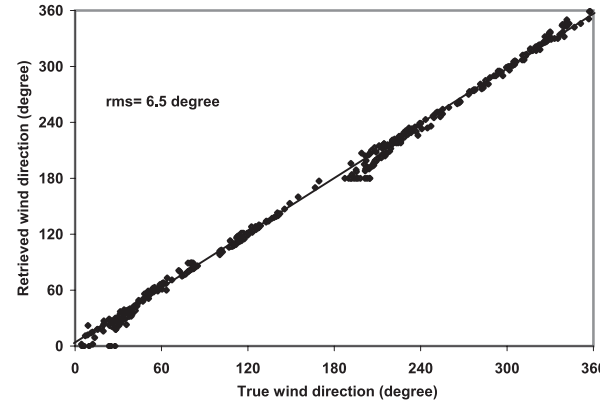

Figure 9. Physical retrieval of the sea surface wind direction for noise-free data. The viewing zenith angle is 53°.

with radiometric noises is 1.4 m s^{-1}. The wind direction product is a new product, and the regression equation for the wind direction is not available yet. However, it is found that the ratio of the third to the fourth Stokes component (except for the zero points of sin 2ϕ) is very successful to separate the regions of the wind direction (Figure 8). The ratio is less than -4 in regions 1 and 4. The ratio is larger than -2 in regions 2 and 3. Furthermore, the third Stokes component is negative in region 1 (0°, 90°) and positive in region 4 (270°, 360°) (see Figure 2). The fourth Stokes component is negative in region 2 (90°, 180°) and positive in region 3 (180°, 270°) (see Figure 2). Thus the ratio of the third and the fourth components and themselves are able to provide the first guess of the wind direction.

[15] The physical retrieval algorithm is tested for the simulated polarimetric data without and with radiometric noise. The simulations are carried out for a global data set from National Center for Environmental Prediction (NCEP). The data with wind speed smaller than 5 m s^{-1} are excluded. The retrieval procedures are to take the first guess for sea surface wind speed and total precipitable water as well as cloud liquid water from the regression method and to then use the third and the fourth Stokes components at 37 GHz to determine the region of the wind direction. The full Stokes components at 37 GHz are used to calculate the sea surface wind direction and speed. At present, retrievals are limited to the case where the magnitude of the third or fourth Stokes component is significant (>0.15 K). With a noise-free data set, the RMS error of the physical retrieval is 6.5 degrees (Figure 9) for sea surface wind direction and 0.3 m s^{-1} (Figure 10) for wind speed.

[16] Radiometric noise is one key factor affecting the retrieval performance [*WindSAT System Requirements Review*, 1997]. The required noise equivalent difference of temperature (NEDT) for each single polarization at 37 GHz is 0.1 K [*WindSAT System Requirements Review*, 1997]. The design of the CMIS sensor is at the same level. The NEDT for a typical single observation is generally much larger than the required value. However, the requirement can be achieved by composing multiple observations. We select the random noise of 0.1 K for the vertically and horizontally polarized brightness temperatures. The NEDT for the third and fourth Stokes components is larger than the first two Stokes components by a factor of the square root of 2. The factor relates to the radiometer design of WindSAT where the third Stokes component is obtained from the measurement at 45° polarization and the measurement at $-45°$ polarization. The fourth component is the difference between the measurements at left-handed circular polarization and the measurement at the right-handed circular polarization. When the noise is taken into account in the

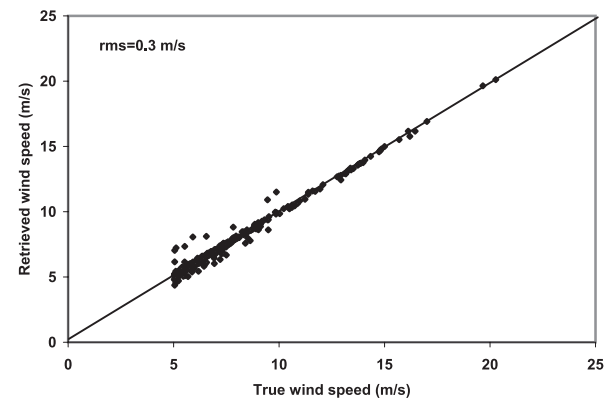

Figure 10. Same as Figure 9, but for sea surface wind speed.

retrieval, the RMS errors increase to 10 degrees (Figure 11) for the wind direction, to 0.6 m s^{-1} (Figure 12) for the wind speed.

5. Discussion

[17] In this study a physical inversion method is presented for the retrieval of sea surface wind vector in the marine environment from passive microwave remote sensing. The algorithm is tested for the wind speed larger than 5 m s^{-1}.

[18] The physical retrieval algorithm is studied and validated against the simulated data. The algorithm performance will be assessed when the real data such as WindSAT and CMIS data are available in the future. The algorithm has a problem to process data where both the third and fourth Stokes components are very small due to the measurement noise. To overcome the problem, one may use the measurement at the vertical and horizontal polarizations only to estimate the wind direction or use the larger signature for the third and the fourth components from the two-azimuthal (e.g., ϕ, $\phi + 45^o$) looking measurements. The polarimetric and the multiple looking observations have been mentioned [*Piepmeier and Gasiewski*, 2001]. The physical retrieval is limited for the wind speed from 5 to 25 m s^{-1} because the surface emissivity model is not reliable for very low and very high speeds. There exist large uncertainties for the wind direction near 40^o and 330^o in Figure 11. The large uncertainties may result from the fact that the radiometric noise changes the sign of the increment of the horizontally polarized brightness temperature there (see Figure 2). It is not clear why the uncertainties near 130^o or near 230^o are relatively small although the increment of the horizontally polarized brightness temperature there is also close to zero. More efforts are needed to improve the retrieval algorithm.

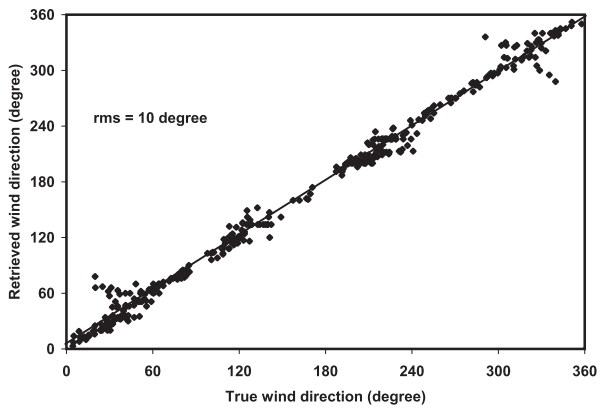

Figure 11. Physical retrieval of the sea wind direction for data with a random error of 0.5 K for the sea surface temperature, the random radiometric noises of 0.1 K and 0.15 K for the first two components and the last two components of Stokes vectors, respectively. The viewing zenith angle is 53°.

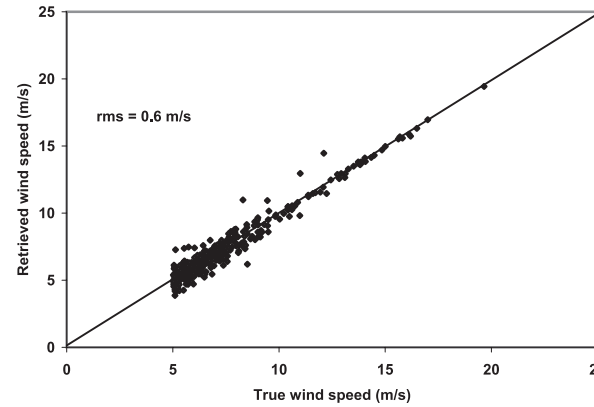

Figure 12. Same as Figure 11, but for sea surface wind speed.

[19] **Acknowledgments.** We would like to thank Xiaofan Li for his helpful comments. This research is supported by NOAA/Integrated Program Office.

References

Butler, J. J., and R. A. Barnes, Calibration strategy for the Earth Observing System (EOS)-AM-1 platform, *IEEE Trans. Geosci. Remote Sens.*, *36*, 1056–1061, 1998.

Chedin, A., N. A. Scott, C. Wahiche, and P. Mouliner, The improved initialization inversion method: A high resolution physical method for temperature retrievals from a satellite of the TIROS-N series, *J. Clim. Appl. Meteorol.*, *24*, 128–143, 1985.

Gasiewski, A., and D. B. Kunkee, Polarized microwave emission from water waves, *Radio Sci.*, *29*, 1449–1466, 1994.

Goodberlet, M. A., C. T. Swift, and J. C. Wilkerson, Ocean surface wind speed measurements of the Special Sensor Microwave/Imager (SSM/I), *IEEE Trans. Geosci. Remote Sens.*, *28*, 823–827, 1990.

Haferman, J. L., W. F. Krajewski, T. F. Smith, and A. Sanchez, Radiative transfer for a three-dimensional raining cloud, *Appl. Opt.*, *32*, 2795–2802, 1993.

Hollinger, J. P., J. L. Peirce, and G. A. Poe, SSM/I instrument evaluation, *IEEE Trans*, *Geosci. Remote Sens.*, *28*, 781–790, 1990.

Kummerow, C., R. A. Mack, and I. M. Hakkarinen, A self-consistency approach to improve microwave rainfall rate estimation from space, *J. Appl. Meteorol.*, *28*, 869–884, 1989.

Liu, Q., and C. Simmer, Retrieval algorithms for Special Sensor Microwave/Imager (SSM/I), *Proc. SPIE*, *3503*, 313–321, 1998.

Liu, Q., and F. Weng, A microwave polarimetric two-stream radiative transfer model, *J. Atmos. Sci.*, *59*, 2396–2402, 2002.

Liu, Q., C. Simmer, and E. Ruprecht, Three-dimensional radiative transfer effects of clouds in the microwave spectral range, *J. Geophys. Res.*, *101*, 4289–4298, 1996.

Meissner, T., and F. Wentz, An updated analysis of the ocean surface wind direction signal in passive microwave brightness temperatures, *IEEE Trans. Geosci. Remote Sens.*, *40*, 1230–1240, 2002.

Petty, G. W., Physical retrievals of over-ocean rain rate from multichannel microwave imagery, part II, Algorithm implementation, *Meteorol. Atmos. Phys.*, *54*, 101–122, 1994.

Piepmeier, J. R., and A. J. Gasiewski, High-resolution passive polarimetric microwave mapping of ocean surface wind vector fields, *IEEE Trans. Geosci. Remote Sens.*, *39*, 606–622, 2001.

Reynolds, R. W., and L. Roberts, Global sea-surface temperature climotology from in-situ, satellite, and ice data, *Trop. Ocean Atmos. Newsl. (CIMAS)*, *37*, 17, 1987.

Schmetz, J., and O. M. Turpeinen, Estimation of the upper troposphere relative humidity field from METEOSAT water vapor image data, *J. Appl. Meteorol.*, *27*, 889–899, 1988.

Simmer, C., *Satellitenfernerkundung Hydrologischer Parameter der Atmosphaere mit Mikrowellen*, 313 pp., Verlag Dr. Kovac, Hamburg, Germany, 1994.

Smith, E. A., A. Mugnai, H. J. Cooper, G. J. Tripoli, and X. Xiang, Foundations for statistical-physical precipitation retrieval from passive microwave satellite measurements, part I, Brightness-temperature properties of a time-dependent cloud-radiation model, *J. Appl. Meteorol.*, *31*, 506–531, 1992.

St. Germain, K., and G. Poe, Polarimetric emission model of the sea at microwave frequencies, part II, Comparison with measurements, report, Nav. Res. Lab., Washington, D. C., 1998.

Weng, F., A multi-layer discrete-ordinate method for vector radiative transfer in a vertically inhomogeneous, emitting and scattering atmosphere, I, Theory, *J. Quant. Spectrosc. Radiat. Transfer*, *47*, 19–33, 1992.

Weng, F., and N. C. Grody, Retrieval of ice cloud parameters using a microwave imaging radiometer, *J. Atmos. Sci.*, *57*, 1069–1081, 2000.

Wentz, F. J., Measurement of the oceanic wind vector using satellite microwave radiometers, *IEEE Trans. Geosci. Remote Sens.*, *30*, 960–972, 1992.

WindSAT System Requirements Review (SRR), December 16–17, 1997. (http://npoesslib.ipo.noaa.gov/Splnotes/CMIS/WSATSRR.PDF)

Yueh, S. H., Modeling of wind direction signals in polarimetric sea surface brightness temperatures, *IEEE Trans. Geosci. Remote Sens.*, *35*, 1400–1418, 1997.

Yueh, S. H., and W. Wilson, Validation of wind radiometer technique using aircraft radiometer and radar measurements for high ocean wind, *Rep. D-17815*, Jet Propul. Lab., Pasaden, Calif., 1999.

Yueh, S. H., W. Wilson, S. Dinardo, and F. Li, Polarimetric brightness signatures of ocean wind direction, *IEEE Trans. Geosci. Remote Sens*, *37*, 949–959, 1999.

Q. Liu, NOAA/NESDIS, 5200 Auth Road, Room 601, Camp Springs, MD 20746, USA. (Quanhua.Liu@noaa.gov)

F. Weng, Office of Research and Applications, NOAA/NESDIS, Camp Springs, MD 20746, USA.